Available online at www.sciencedirect.com

ScienceDirect

Mendeleev Commun., 2023, **33**, 58–60

Mendeleev Communications

Luminescent and photocatalytic properties of a 6-connected msw-type 3D Cd^{II} metal–organic framework

Bing Wang, Yan-Peng Li, Pei-Ran Wang, Xiao-Gang Wang, Yuan-Yuan Liu, Hong-Da Wu and Yan-Jun Meng*

Hebei Vocational University of Industry and Technology, 050091 Shijiazhuang, Hebei, China.
E-mail: yan_jun_meng@163.com

DOI: 10.1016/j.mencom.2023.01.018

Hydrothermal reactions of H_6bhc and $Cd(NO_3)_2{\cdot}4H_2O$ produced a new Cd^{II} compound $[Cd_3(bhc)(H_2O)_8]_n$ (H_6bhc = benzene-1,2,3,4,5,6-hexacarboxylic acid). Single crystal X-ray diffraction analysis revealed that this compound features a 3D framework with bhc^{6-} ligands in a μ_6-bridging mode. Its luminescent and photocatalytic properties were explored.

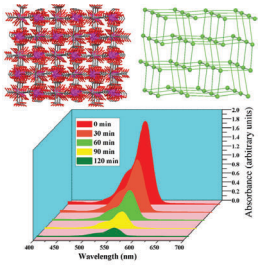

Used as photocatalyst for the degradation of Rhodamine B

Keywords: Cd^{II} compound, hydrothermal synthesis, 3D framework, luminescence, photocatalysis.

Due to the rapid development of chemical industry, large amounts of wastewater containing organic dyes, which are chemically stable and unbiodegradable, were discharged into the environment without any pretreatment to cause serious harm to human health.[1–3] Photocatalytic technology employing clean solar energy is a highly efficient method for the degradation of organic dyes without secondary pollution,[4–6] and nanocatalysts including metal oxide and metal sulfide nanoparticles have been synthesized and exploited as photocatalysts for the remediation of dye wastewater. However, low separation efficiency and fast recombination of electron–hole pairs limit their practical application.[7,8] Therefore, the development of new photocatalytic materials for the degradation of organic dyes is a problem of considerable current importance. Recently, metal–organic frameworks (MOFs) that can absorb UV or visible light have been synthesized and applied as photocatalysts for the degradation of organic dye molecules with high degradation efficiency.[9–12] The introduction of organic ligands made electron–hole separation more efficient and recombination more difficult.[13] This advantage of MOFs over traditional photocatalysts encouraged us to develop new active MOFs-based photocatalysts.

In this work, we selected a hexacarboxylic acid ligand, benzene-1,2,3,4,5,6-hexacarboxylic acid (H_6bhc), to react with $Cd(NO_3)_2{\cdot}4H_2O$ under hydrothermal conditions.† The connection of bhc^{6-} and Cd^{II} ions resulted in a 3D framework representing a 6-connected msw topological network. Note that this compound exhibited high photocatalytic activity for the degradation of Rhodamine B (RhB) under UV light irradiation.

The X-ray diffraction analysis‡ revealed that compound **1** crystallizes in the orthorhombic space group *Pbca* and exhibits a 3D framework with 6-connected msw topology. Each asymmetric unit of **1** consists of three Cd^{II} ions, one bhc^{6-} ligand, and eight coordinated water ligands. Figure 1(*a*) shows that Cd1 and Cd2 are six-coordinated with a distorted octahedral geometry, while Cd3 is eight-coordinated with a distorted monocapped pentagonal bipyramidal geometry. The octahedrons of Cd1 and Cd2 are constituted by four carboxylate oxygen atoms and two water ligands, and the coordination polyhedron of Cd3 is formed by four carboxylate oxygen atoms and four water ligands. The Cd–O distances around the above Cd^{II} polyhedrons are in a range of 2.218(3)–2.567(3) Å, and they are comparable with those reported for Cd^{II}–carboxylate coordination polymers.[14,15] In a self-assembly process, H_6bhc was completely deprotonated, and each bhc^{6-} ligand was coordinated to six Cd^{II} ions with its deprotonated carboxylate groups in a uniform chelating mode [Figure 1(*b*)]. Finally, all Cd^{II} ions are bridged by the polydentate bhc^{6-} ligands together to construct a new 3D framework

† *Preparation of* $[Cd_3(bhc)(H_2O)_8]_n$ **1**. A mixture of $Cd(NO_3)_2{\cdot}4H_2O$ (154 mg, 0.5 mmol), H_6bhc (34 mg, 0.1 mmol), $NaHCO_3$ (50 mg, 0.6 mmol), and 12 ml of H_2O was sealed in a 23 ml Teflon-lined stainless steel autoclave and heated at 150 °C for 3 days. After cooling to room temperature, colorless block crystals were obtained by filtration, and the yield was 46% based on H_6bhc. Calc. for $C_{12}H_{16}Cd_3O_{20}$ (%): C, 17.63; H, 1.97. Found (%): C, 17.67; H, 1.94. IR (KBr pellet): 3442 (s), 1577 (s), 1552 (m), 1476 (s), 1400 (s), 1223 (s), 1159 (w), 1096(m), 1045 (w), 956 (m), 867 (m), 804 (m), 778 (w), 728 (w), 664 (w).

‡ *Crystal data for* **1**. $C_{12}H_{16}Cd_3O_{20}$, M = 817.48, orthorhombic, space group *Pbca*, a = 13.4137(7), b = 13.3410(6) and c = 22.8404(13) Å, $\alpha = \beta = \gamma$ = 90°, V = 4087.3(4) Å^3, Z = 8, D_{calc} = 2.657 g cm^{-3}, μ = 3.198 mm^{-1}, $F(000)$ = 1368, T = 293(2) K, 30112 reflections measured, 4679 independent reflections (R_{int} = 0.0270), final R_1 [$I > 2\sigma(I)$] = 0.0333, wR_2 = 0.0606, GOF = 1.142. The crystal data were collected on a computer-controlled Rigaku Mercury CCD diffractometer with graphite-monochromated MoKα radiation (λ = 0.71073 Å). The structure was solved by direct methods, and all nonhydrogen atoms were refined anisotropically with SHELXTL using full-matrix least-squares procedures based on F^2 values.[23] Hydrogen atom positions were fixed geometrically at their identical positions.

CCDC 2204500 contains the supplementary crystallographic data for this paper. These data can be obtained free of charge from The Cambridge Crystallographic Data Centre *via* http://www.ccdc.cam.ac.uk.

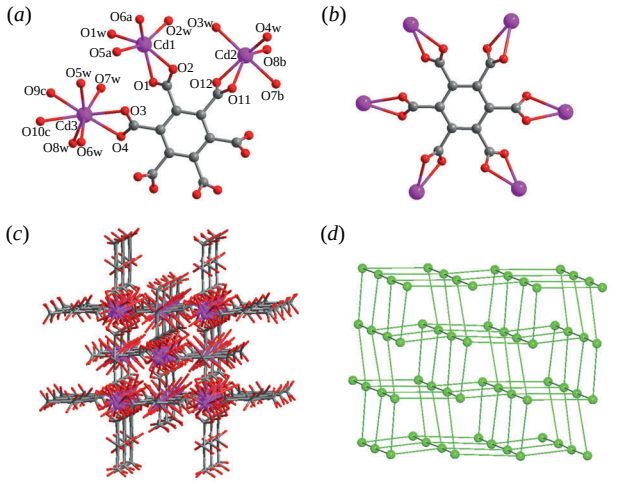

Figure 1 (*a*) Coordination environments of Cd^{II} ions in molecule of **1**; (*b*) coordination mode of the bhc^{6-} ligand; (*c*) the 3D framework of **1**; and (*d*) 6-connected msw topological network for **1**.

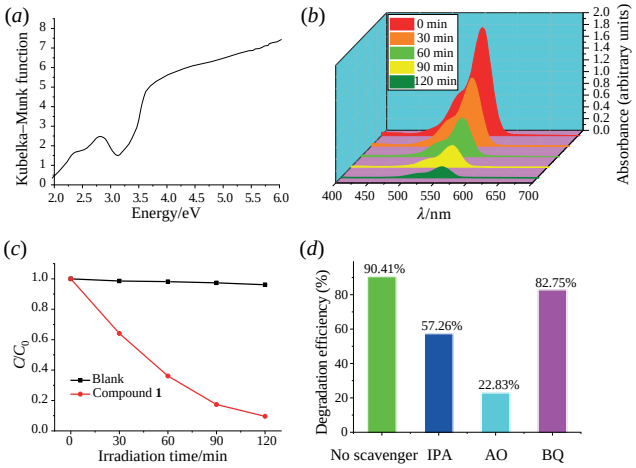

Figure 2 (*a*) Solid-state optical diffuse-reflectance spectrum of compound **1**; (*b*) UV-VIS absorption spectra of RhB in the presence of **1** at different irradiation times; (*c*) efficiencies of the photocatalytic degradation of RhB solution with and without a photocatalyst; and (*d*) efficiencies of the photocatalytic degradation of RhB in solution in the presence of compound **1** and scavengers (IPA, AO, and BQ).

[Figure 1(*c*)]. In this 3D framework, the bhc^{6-} ligands can be topologically simplified into 6-connected nodes, and the central Cd^{II} ions can be viewed as linear connectors. As a result, the whole 3D framework of **1** can be reduced into a 6-connected msw topological network with the point symbol of $\{4^8.6^7\}$ [Figure 1(*d*)]. According to published data, most of the reported 6-connected MOFs are classified as pcu topological networks.[16,17] To the best of our knowledge, 6-connected MOFs exhibiting msw topology were rarely reported.

Taking into account the excellent luminescence emission properties of coordination polymers based on Cd^{II} or Zn^{II} ions,[18–21] we measured the solid-state emission spectra of **1**, desolvated samples, and H_6bhc at room temperature. As shown in Figure S2 (see Online Supplementary Materials), compound **1** exhibits a broad emission band with a maximum at 488 nm (λ_{ex} = 380 nm), and the free H_6bhc ligand shows an emission band at 437 nm (λ_{ex} = 380 nm). The emission spectrum of **1** has a significant red shift of 51 nm compared to that of the free H_6bhc ligand, which can be caused by the coordination of bhc^{6-} ligands to Cd^{II} ions, which can effectively increase the rigidity of the hhc^{6-} ligand and thus reduce the nonradiative energy decay. After the removal of coordinated water molecules from the 3D framework, the desolvated samples showed stronger luminescence than that of **1**, revealing that the coordinated water molecules can quench luminescence owing to high energy O–H oscillators.[22] The quantum yields of compound **1** and the desolvated compound measured at room temperature were 31.28 and 38.82%, respectively. Note that, according to the PXRD pattern shown in Figure S1(*a*), the solvent-free sample kept good structural integrity.

The potential semiconductor nature of **1** was demonstrated by its optical diffuse reflectance spectrum. According to Figure 2(*a*), the extrapolation of a linear portion of the absorption edge gave a band gap energy of 3.12 eV for **1**, indicating that compound **1** can serve as a photocatalyst for the removal of toxic organic dyes. Rhodamine B (RhB) was chosen as a model dye to evaluate the photocatalytic performance of **1** under UV light irradiation. Figure 2(*b*) shows that the maximum absorption peak of RhB at 554 nm decreased with irradiation time, and the efficiency of RhB degradation reached 90.41% after 120 min [Figure 2(*c*)]. A control experiment without compound **1** was also carried out under the same conditions, and the efficiency of RhB degradation was only 3.90% to demonstrate the good photocatalytic activity of **1** for the degradation of RhB [Figure 2(*c*)]. After the degradation, the structure of compound **1** showed no obvious changes compared to that of the pristine samples [Figure S1(*a*)]; thus, compound **1** as a photocatalyst can be recycled. We also investigated the photocatalytic mechanism of RhB degradation by compound **1** in radical capture experiments. Isopropanol (IPA), ammonium oxalate (AO), and benzoquinone (BQ) were selected as scavengers for hydroxyl radicals (•OH), holes (h^+), and superoxide radicals ($•O^{2-}$), respectively, in the photocatalytic processes. According to Figure 2(*d*), in the presence of IPA and AO, the degradation efficiencies decreased from 90.41 to 57.26 and 22.83%, respectively, indicating that the •OH and h^+ were the main active species for RhB degradation; in the presence of BQ, the degradation efficiency decreased from 90.41 to 82.75%, suggesting that the $•O^{2-}$ radicals made a little contribution to RhB degradation. Thus, a plausible degradation mechanism can be described as shown in Figure S3: when the solid particles of **1** are excited by UV light, electrons from the valence band can escape to the conductive band and produce electron–hole pairs. The generated holes (h^+) and photogenerated electrons (e^-) can react with water and oxygen to form hydroxyl radicals (•OH), which can effectively degrade organic dyes into harmless products. In addition, we also studied the stability of **1** as a photocatalyst in cyclic experiments and found that the efficiency of RhB degradation by **1** was higher than 89% after three cycles (Figure S4).

In summary, we synthesized a new 3D Cd^{II} compound as a 6-connected msw topological network by the hydrothermal reactions of $Cd(NO_3)_2·4H_2O$ and H_6bhc. This compound can be used as a photocatalyt to degrade RhB irradiated by UV light.

This work was supported by Hebei Vocational University of Industry and Technology.

Online Supplementary Materials

Supplementary data (a table of bond parameters, PXRD patterns, TGA curves, luminescent emission spectra, and a schematic diagram of degradation mechanism) associated with this article can be found in the online version at doi: 10.1016/j.mencom.2023.01.018.

References

1 C.-C. Wang, J.-R. Li, X.-L. Lv, Y.-Q. Zhang and G. Guo, *Energy Environ. Sci.*, 2014, **7**, 2831.
2 S. Qu, J.-P. Zhang, G.-Q. Kong and C.-D. Wu, *Dalton Trans.*, 2015, **44**, 7862.

3 L. Qin, Q. Hu, Y. Wu, J.-L. Cai and Y.-Y. Li, *CrystEngComm*, 2018, **20**, 4042.
4 L.-L. Shi, T.-R. Zheng, M. Li, L.-L. Qian, B.-L. Li and H.-Y. Li, *RSC Adv.*, 2017, **7**, 23432.
5 H. Zhu, D. Liu, Y.-H. Li and G.-H. Cui, *Transition Met. Chem*., 2020, **45**, 19.
6 R.-Y. Zhao, R.-D. Xu, G.-N. Liu, Y. Sun and C. Li, *Inorg. Chem. Commun.*, 2019, **105**, 135.
7 M. Sharma, T. Jain, S. Singh and O. P. Pandey, *Sol. Energy*, 2012, **86**, 626.
8 I. K. Konstantinou and T. A. Albanis, *Appl. Catal., B*, 2004, **49**, 1.
9 X. Lu, Y. Zhao, X.-L. Wang, G.-C. Liu, N. Xu, H.-Y. Lin and X. Wang, *CrystEngComm*, 2021, **23**, 3828.
10 J. Zhao, X. Wang and P. Dai, *J. Mol. Struct.*, 2021, **1235**, 130220.
11 J. Zhao, W.-W. Dong, Y.-P. Wu, Y.-N. Wang, C. Wang, D.-S. Li and Q.-C. Zhang, *J. Mater. Chem. A*, 2015, **3**, 6962.
12 S. Mirdya, T. Basak and S. Chattopadhyay, *Polyhedron*, 2019, **170**, 253.
13 J. Cheng, T. Hu, W. Li, Z. Chang and C. Sun, *J. Solid State Chem.*, 2020, **282**, 121125.
14 X.-Y. Cao, J. Zhang, Z.-J. Li, J.-K. Cheng and Y.-G. Yao, *CrystEngComm*, 2007, **9**, 806.
15 R.-P. Ye, X. Zhang, J.-Q. Zhai, Y.-Y. Qin, L. Zhang, Y.-G. Yao and J. Zhang, *CrystEngComm*, 2015, **17**, 9155.
16 Y.-J. Liang, J. Yao, M. Deng, Y.-E. Liu, Q.-Q. Xu, Q.-X. Li, B. Jing, A.-X. Zhu and B. Huang, *CrystEngComm*, 2021, **23**, 7348.
17 R. An, X. Wang, H.-M. Hu, Z. Zhao, C. Bai and G. Xue, *CrystEngComm*, 2015, **17**, 8289.
18 X.-J. Wei, Y.-H. Li, Z.-B. Qin and G.-H. Cui, *J. Mol. Struct.*, 2019, **1175**, 253.
19 C. Wang, Z. Zhang, L. Zhang, F. Li and X. Zhou, *Sci. China: Chem.*, 2010, **53**, 2079.
20 Z.-Z. Shi, Z.-R. Pan, H.-L. Jia, S.-G. Chen, L. Qin and H.-G. Zheng, *Cryst. Growth Des.*, 2016, **16**, 2747.
21 J. Pan, F.-L. Jiang, M.-Y. Wu, L. Chen, J.-J. Qian, K.-Z. Su, X.-Y. Wan and M.-C. Hong, *CrystEngComm*, 2014, **16**, 11078.
22 D.-L. Yang, X. Zhang, Y.-G. Yao and J. Zhang, *CrystEngComm*, 2014, **16**, 8047.
23 G. M. Sheldrick, *Acta Crystallogr., Sect. C: Struct. Chem.*, 2015, **71**, 3.

Received: 8th July 2022; Com. 22/6950